

# Training Multimodal Large Reasoning Models Needs Better Thoughts: A Three-Stage Framework for Long Chain-of-Thought Synthesis and Selection

Yizhi Wang<sup>1,2</sup>, Linan Yue<sup>1,2,\*</sup>, Min-Ling Zhang<sup>1,2,\*</sup>

School of Computer Science and Engineering, Southeast University<sup>1</sup>

Key Laboratory of Computer Network and Information Integration (SEU), Ministry of Education<sup>2</sup>  
Nanjing 210096, China

wang-yz@seu.edu.cn, lnyue@seu.edu.cn, zhangml@seu.edu.cn

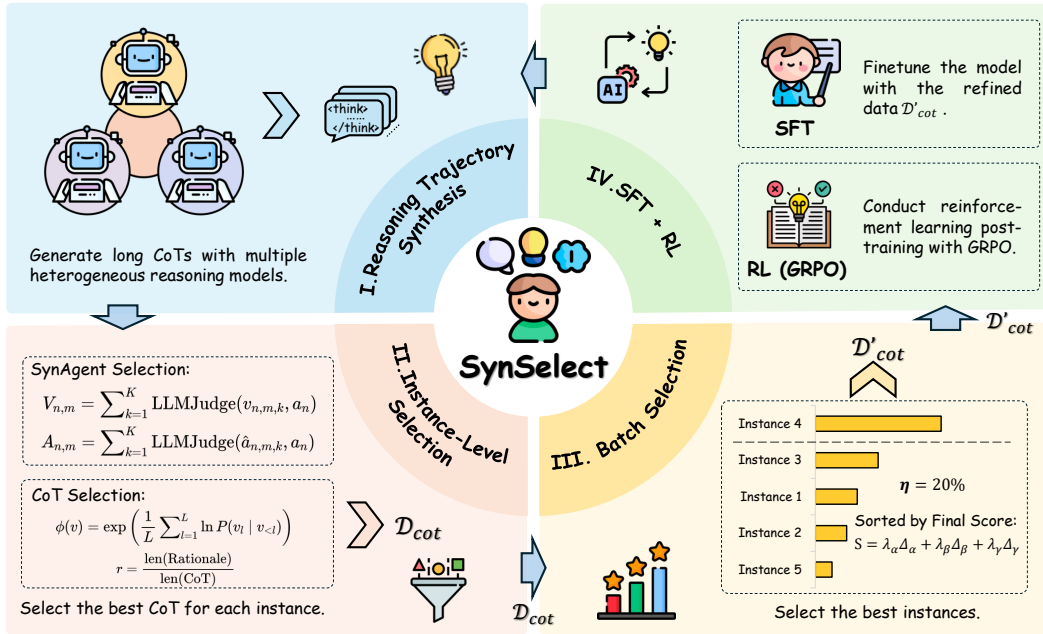


Figure 1. Overview of the *SynSelect* pipeline. *SynSelect* first generates high-quality multimodal CoT data in three stages: (I) Reasoning trajectory synthesis: multiple heterogeneous MLRMs generate candidate CoTs; (II) Instance-level selection: the best CoT is picked for each question; (III) Batch selection: an optimal subset is selected from all instances. Then, in (IV), the synthesized dataset is used for SFT, followed by RL post-training to further enhance multimodal reasoning capabilities. Finally, the trained model can subsequently be reused as a new MLRM in Stage (I), enabling iterative data synthesis while keeping the training procedure decoupled from *SynSelect*.

## Abstract

Large Reasoning Models (LRMs) have demonstrated remarkable performance on complex reasoning tasks through long Chain-of-Thought (CoT) reasoning. Extending these successes to multimodal reasoning remains challenging due to the increased complexity of integrating diverse input modalities and the scarcity of high-quality long CoT training data. Existing multimodal datasets and CoT synthesis

methods still suffer from limited reasoning depth, modality conversion errors, and rigid generation pipelines, hindering model performance and stability. To this end, in this paper, we propose *SynSelect*, a novel three-stage Synthesis-Selection framework for generating high-quality long CoT data tailored to multimodal reasoning tasks. Specifically, *SynSelect* first leverages multiple heterogeneous multimodal LRMs to produce diverse candidate CoTs, and then applies both instance and batch level selection to filter high-quality CoTs that can effectively enhance the model’s reasoning capabilities. Extensive experiments on multiple multimodal

\*Corresponding authors.

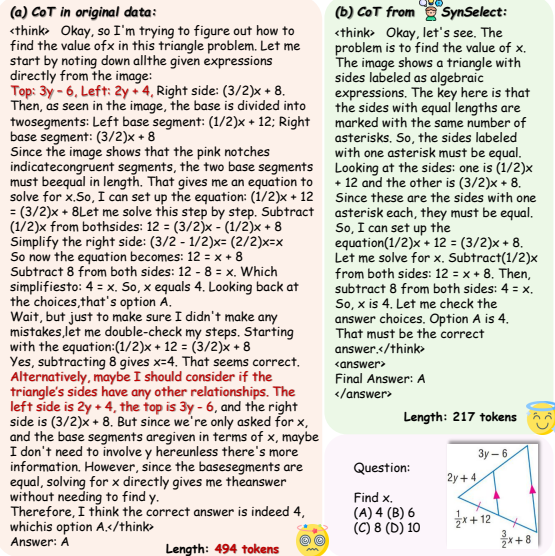


Figure 2. Example of *SynSelect* data. *SynSelect* produces shorter and more accurate CoTs compared with the original data, reducing redundancy and errors through its synthesis–selection framework. More examples could be found in appendix.

benchmarks demonstrate that models supervised fine-tuned on *SynSelect*-generated data significantly outperform baselines and achieve further improvements after reinforcement learning post-training. Our results validate *SynSelect* as an effective approach for advancing multimodal LLMs reasoning capabilities. Code and synthesized dataset are available at <https://github.com/Snowstorm1492/SynSelect>.

## 1. Introduction

Large Reasoning Models (LRMs), such as DeepSeek-R1 [6], have exhibited exceptional capabilities in complex reasoning tasks, attributed to the application of large-scale reinforcement learning (RL) post-training in language models [6, 7, 22, 26, 37, 39]. These models typically employ structured long Chain-of-Thought (CoT) reasoning, enhanced by mechanisms of self-reflection and self-correction, which significantly improve their logical reasoning and decision-making abilities. Inspired by this success, researchers have begun exploring the extension of LRMs training paradigms to the multimodal domain. However, existing studies reveal that current multimodal LRMs (MLRMs) still face challenges in terms of both performance and stability [11, 16, 21, 40, 44, 45]. This is primarily due to the increased architectural complexity and training difficulty associated with integrating diverse modalities, such as language and vision. Under such conditions, RL post-training often fails to converge stably in multimodal settings and may even lead to

performance degradation, ultimately hindering the model’s effectiveness in complex reasoning tasks.

To mitigate these challenges, a promising strategy is to first employ supervised fine-tuning (SFT) methods on long CoTs to improve the model’s basic reasoning ability, followed by RL-based optimization to further boost performance [3, 4, 11, 23, 40]. This two-stage paradigm has proven effective in text-only settings. However, extending it to multimodal reasoning introduces new obstacles. Specifically, multimodal reasoning demands precise alignment between visual content and linguistic logic at every step, making model performance highly sensitive to the quality of SFT data. Unfortunately, existing multimodal datasets generally lack high-quality, long CoT annotations. For example, as shown in Figure 2 (a), they could contain CoTs that are verbose or invalid. Current benchmarks (e.g., the multimodal subset of MMLU [10], MMBench [17], ScienceQA [18]) focus on basic tasks and offer limited support for complex reasoning chains. Furthermore, prevailing CoT synthesis approaches also encounter several limitations. Some methods first convert visual inputs into textual descriptions and then apply models like DeepSeek-R1 for CoT generation, which may introduce cascading errors due to modality conversion [11, 40]. Others, such as LLaVA-CoT [38], generate CoTs in fixed stages, often resulting in rigid and less flexible reasoning processes.

To this end, in this paper, we propose *SynSelect*, a three-stage **Synthesis-Selection** framework designed to generate high-quality long CoT data tailored for multimodal reasoning tasks. The framework contains three step-wise stages: Synthesis, Initial Filtering, and Refined Selection, aiming to construct training data for the SFT of MLRMs. Specifically, **in the Synthesis stage**, given a dataset of  $N$  instances, *SynSelect* leverages  $M$  heterogeneous MLRMs to perform  $K$  independent samplings per instance, yielding  $M \times K$  diverse reasoning paths. By exploiting architectural diversity and sampling variance, *SynSelect* significantly enhances the coverage and diversity of candidate CoTs. **During the Initial Filtering stage**, *SynSelect* applies multi-dimensional evaluation metrics in the instance-level selection, including answer correctness, reasoning validity, and length appropriateness, to assess the quality of each candidate CoT. It then selects the most semantically clear and logically coherent reasoning path for each instance. **In the Refined Selection stage**, *SynSelect* adopts a batch selection strategy, introducing query-aware and CoT-aware selection to identify the most instructive  $N'$  samples from the original  $N$  instances. These samples are optimized for boosting reasoning capabilities, achieving a balance between training efficiency and model performance. The final output is a high quality dataset specifically curated for complex multimodal reasoning. As shown in Figure 2 (b), *SynSelect* ultimately produces concise, accurate, and well-structured CoTs.

Our contributions are summarized as follows:

- We propose *SynSelect*, a three-stage synthesis-selection framework to generate high-quality long CoT data tailored for multimodal reasoning tasks.
- In the synthesis stage, we employ multiple heterogeneous MLRMs to generate long CoTs, effectively leveraging architectural diversity to produce more comprehensive and diverse reasoning paths.
- We design multi-level selection strategies at both the instance and batch levels, enabling fine-grained control over CoT quality. The selected samples can contribute to improving reasoning capabilities.
- Extensive experiments are conducted on multiple multimodal benchmark datasets. Results show that models supervised fine-tuned on *SynSelect*-generated long CoT data outperform various baselines on complex reasoning tasks. Besides, models fine-tuned with *SynSelect* data achieve additional gains after RL post-training compared to models trained solely with RL. These findings validate the effectiveness of *SynSelect*-generated data.

## 2. Related Works

**Multimodal Large Reasoning Models.** In recent years, Multimodal Large Language Models (MLLMs) have attracted considerable attention and achieved promising results across a range of tasks [1, 5, 9, 12, 15, 31, 32, 36, 38, 43, 46]. However, these models often lack explicit long Chain-of-Thought (CoT) reasoning mechanisms [1, 5, 9, 32, 36], which poses significant challenges when tackling complex tasks that require multi-step reasoning. Inspired by the continual progress of LLMs in reasoning (e.g., DeepSeek-R1), which enhances reasoning strategies via large-scale RL post-training, researchers have begun to focus on developing MLRMs [8, 14, 25, 28, 29, 33, 35, 41, 47]. Current reasoning models can be broadly categorized into two types: (1) RL-based training approaches [3, 21, 23, 33, 47, 49]. These methods (e.g., MM-Eureka [21] and VisualThinker R1 [49]) directly employ RL methods to train models for better reasoning capabilities. While promising, they often suffer from issues such as shallow reasoning trajectories [11, 21], visual hallucinations [33], and ineffective length-based rewards [49], leading to sub-optimal reasoning quality and generalization. (2) SFT+RL approaches [4, 11, 30, 40]. These methods (e.g., R1-OneVision [40] and Vision-R1 [11]) typically rely on converting visual inputs into intermediate textual representations, such as natural language or code, which are then fed into LRMs to generate long CoTs for SFT. RL is then applied on top of these fine-tuned models. However, such conversion pipelines are prone to losing or distorting crucial visual information, which may degrade the accuracy and consistency of the synthesized long CoTs, ultimately impairing the model’s performance.

**Multimodal Reasoning Datasets Construction.** Constructing high-quality multimodal reasoning datasets is crucial for enabling complex reasoning capabilities in models. Early datasets (e.g., ChartQA [20], MMBench [17], and ScienceQA [18]) primarily focus on foundational tasks like visual question answering and chart understanding. While these datasets exhibit a certain degree of complexity, they generally lack explicit long CoT reasoning processes, making it difficult for models to perform multi-step reasoning. To address this limitation, researchers have explored automatic methods [34, 38, 42] for constructing multimodal reasoning data. For example, LLava-CoT-100K [38] leverages staged prompting with GPT-4o to generate reasoning CoT composed of four structured components: Summary, Caption, Reasoning, and Conclusion. This improves the alignment between visual content and language-based reasoning. However, its rigid, predefined reasoning structure limits the model’s ability to generate flexible and diverse reasoning paths. More recent approaches introduce text-based reasoning models to improve the quality of multimodal CoT generation [2, 11, 40]. For example, R1-OneVision-Dataset [40] first translates images into formal representations (e.g., matplotlib code), which are then processed by LRMs to generate CoTs. Vision-R1-Cold [11] employs modality bridging techniques to convert visual inputs into natural language, indirectly guiding the reasoning process. While such methods improve the quality of synthesized CoTs, they still face challenges: the vision-to-text conversion may lose critical details or introduce semantic errors, leading to inconsistencies between the CoT and the original visual content, which undermines the accuracy and stability of the reasoning chain. To overcome these limitations, in this paper, we propose *SynSelect*, a long CoT synthesis-selection framework tailored for multimodal reasoning tasks.

## 3. Problem Definition

In this section, we formally define the problem addressed in this paper. Specifically, given a raw multimodal dataset  $\mathcal{D}_{\text{raw}} = \{(q_n, a_n) | 1 \leq n \leq N, n \in \mathbb{N}_+\}$ , where each input query  $q_n$  consists of a pair (query, image), and  $a_n$  denotes the corresponding answer, our objective is two-fold:

- **Reasoning Data Construction:** Augment each raw sample with a long CoT reasoning path with “*aha memont*”, resulting in a new dataset:

$$\mathcal{D}_{\text{cot}} = \{(q_n, a_n, \text{CoT}_n) | 1 \leq n \leq N, n \in \mathbb{N}_+\}. \quad (1)$$

- **Subset Refinement:** Select a high-quality subset of  $\mathcal{D}_{\text{cot}}$  with size  $N' \ll N$ , leading to a compact but informative reasoning dataset:

$$\mathcal{D}'_{\text{cot}} = \{(q_n, a_n, \text{CoT}_n) | 1 \leq n \leq N', n \in \mathbb{N}_+\}, \quad (2)$$

where we define the selection ratio as  $\eta = N'/N$ .

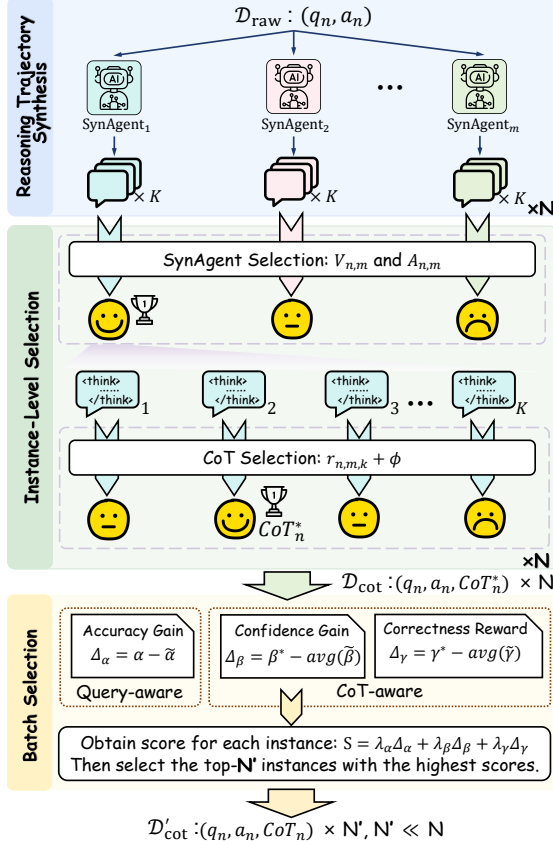


Figure 3. Architecture of the proposed *SynSelect* framework, including Reasoning Trajectory Synthesis, Instance-level Selection, and Batch Selection.  $avg(\cdot)$  denotes the average computed over both  $M$  and  $K$ . Detailed calculation is in Section 4.3.2.

Based on the constructed dataset, we perform SFT on MLLMs to enhance their reasoning capabilities. Besides, RL methods (e.g., GRPO [27]) can be applied to the SFT-tuned models, ultimately yielding MLRMs with stronger step-by-step reasoning abilities.

## 4. Methodology

In this section, as shown in Figure 3, we present the details of our proposed *SynSelect* framework, which consists of three sequential stages:

**1. Synthesis Stage: Reasoning Trajectory Synthesis.** For each instance in the raw multimodal dataset  $\mathcal{D}_{\text{raw}}$ , we first generate a set of diverse long CoT reasoning paths.

**2. Initial Filtering Stage: Instance-level Selection.** We then select the most appropriate reasoning path for each instance from its all CoT candidates. This stage takes both the generated CoTs and the original dataset  $\mathcal{D}_{\text{raw}}$  as input and yields the full multimodal reasoning dataset  $\mathcal{D}_{\text{cot}}$ .

**3. Refined Selection Stage: Batch Selection.** We perform selection at the dataset level. Specifically, we treat

the entire dataset as a batch and take  $\mathcal{D}_{\text{cot}}$  as input to identify a refined subset  $\mathcal{D}'_{\text{cot}} \subset \mathcal{D}_{\text{cot}}$ , consisting of high-quality reasoning samples that are most beneficial for training MLRMs.

### 4.1. Reasoning Trajectory Synthesis

To generate long CoTs for each instance, a straightforward approach is to directly leverage existing MLRMs for generation. However, current MLRMs exhibit diverse capability profiles, with varying strengths across different tasks. To avoid over-reliance on a single model’s behavior, we employ a set of  $M$  heterogeneous MLRMs as *synthesis agents*, denoted as  $\text{SynAgent}_m(\cdot)$ , to collaboratively generate CoTs.

Specifically, for each  $q_n$ , each  $\text{SynAgent}_m(\cdot)$  performs  $K$  rounds of inference with different random seeds  $\varepsilon_{n,m,k}$ :

$$(\text{CoT}, \hat{a})_{n,m,k} = \text{SynAgent}_m(q_n; \varepsilon_{n,m,k}), \quad (3)$$

where  $\hat{a}$  is the model’s predicted answer, and CoT denotes the corresponding reasoning path. Performing  $K$  rounds of sampling allows us to better explore the model’s reasoning space, yielding diverse reasoning trajectories. In this way, we can obtain  $M \times K$  reasoning paths per instance, resulting in a total of  $N \times M \times K$  CoTs across the entire dataset.

**Remark.** All *synthesis agents* used in this stage are native MLRMs (e.g., R1-OneVision [40], MM-Eureka [21] and Vision-R1 [11]). Compared to template-based or vision-text concatenation approaches, these models exhibit more flexible reasoning processes and emergent behaviors such as self-reflection. Furthermore, their native multimodal support enables more effective modality fusion and avoids the risk of information loss that may arise during intermediate modality conversion (e.g., image-to-caption).

### 4.2. Instance-level Selection

Although the synthesized candidate pool contains a substantial number of high-quality CoTs, the majority remain ordinary or suboptimal. Therefore, it is essential to identify the most appropriate reasoning path for each instance. However, evaluating the quality of CoTs is inherently challenging. In our setting, the primary objective is to ensure that the selected CoTs contribute effectively to the SFT of MLLMs. To this end, we design three key indicators to guide the selection process: (1) *Answer correctness*, (2) *Reasoning validity*, and (3) *Length appropriateness*.

Based on these indicators, a straightforward selection strategy for each query is to aggregate all  $M \times K$  CoTs and directly choose the best one. However, our preliminary experiments revealed that CoTs generated by the same *synthesis agent* tend to exhibit higher semantic similarity. For a given query, identifying the agent that performs best often leads to more reliable CoT selection. Therefore, we adopt

a hierarchical instance-level selection strategy. Specifically, for each instance:

- **SynAgent Selection:** We first identify the best-performing agent  $\text{SynAgent}_{m^*}$  based on the defined indicators.
- **CoT Selection:** Then, we select the optimal reasoning path  $k^*$  from the  $K$  CoTs generated by agent  $\text{SynAgent}_{m^*}$ .

Below, we introduce the designed indicators, followed by details of our hierarchical instance-level selection strategy.

#### 4.2.1. Key Indicators of Instance-level Selection

In this subsection, we define three key indicators:

**(1) Answer Correctness** Answer correctness is a foundational guarantee for CoT quality. In this indicator, we use a LLM Judge to verify whether the predicted answer  $\hat{a}$  is consistent with the ground-truth answer  $a$ :

$$\text{LLMJudge}(\hat{a}, a) = \begin{cases} 1 & \text{if } \hat{a} \text{ is consistent with } a, \\ 0 & \text{others.} \end{cases} \quad (4)$$

If the answer associated with a CoT is incorrect (i.e.,  $\text{LLMJudge}(\hat{a}, a) = 0$ ), the CoT is immediately discarded. Otherwise, it is retained for further evaluation.

**(2) Reasoning Validity** Our preliminary experiments revealed that several CoTs yield correct final answers but contain problems such as flawed causal logic and inaccurate visual grounding. Incorporating such CoTs into the SFT training set may degrade model performance, making it essential to identify and remove them. To address this, we propose a novel method for verifying reasoning validity. Specifically, we leverage a small-scale, non-reasoning model (e.g., Qwen2.5-VL-3B [1]), referred to as the LLMPlayer, and examine whether it can correctly solve the problem when aided by a specific CoT generated by the synthesis agents. The intuition is that a reliable CoT should provide effective guidance and improve the performance of a weaker model.

It is worth noting that this step aims to perform a coarse-grained filtering of *potentially unreliable CoTs*. We adopt the assumption: If the LLMPlayer fails to produce the correct answer when provided with a CoT, the CoT is likely to be unreliable. Conversely, if the LLMPlayer succeeds with the CoT, even if it could answer correctly without it, we tentatively consider the CoT to be reliable. A more fine-grained selection process will be conducted in subsequent stages.

This verification process allows us to indirectly evaluate the quality of CoTs through their influence on model behavior, without explicitly dissecting their internal logic. Formally, we define the output and confidence score of the

LLMPlayer, which are further utilized in the hierarchical instance-level selection strategy:

$$v_{n,m,k} = \text{LLMPlayer}(q_n, \text{CoT}_{n,m,k}; \varepsilon_{n,m,k}), \quad (5)$$

where  $v_{n,m,k}$  is the output answer generated by the LLMPlayer. The corresponding confidence score is defined as:

$$\phi(v) = \exp\left(\frac{1}{L} \sum_{l=1}^L \ln P(v_l | v_{<l})\right), \quad (6)$$

where  $\phi(v)$  represents the sequence-level confidence of the generated answer  $v$  (e.g.  $v_{n,m,k}$ ), computed as the exponential of the average log-likelihood over the sequence length  $L$ .

**(3) Length Appropriateness** In practice, we observe that existing MLRMs tend to generate overly verbose CoTs for certain questions. These CoTs often include not only useful reasoning steps but also redundant self-verifications and meaningless repetitions. Given the limited reasoning capabilities of current multimodal models, assessing the redundancy of a CoT becomes particularly important.

However, although some CoTs are excessively long, complex questions inherently require more elaborate reasoning, rendering simple length-based filtering ineffective. To strike a balance, we propose a discrimination method based on the rationale ratio. Specifically, we employ a LLM-based Extractor to identify the core reasoning steps (i.e., the Rationale) within each CoT, and then compute the ratio between the rationale length and the total CoT length:

$$r = \frac{\text{len(Rationale)}}{\text{len(CoT)}}, \quad (7)$$

where a higher ratio  $r$  indicates that the CoT contains denser reasoning content and less redundancy.

#### 4.2.2. Hierarchical Instance-level Selection Strategy

After defining the above indicators, we proceed to select the high-quality CoT for each instance. As previously mentioned, in SynAgent Selection, we begin by selecting the best-performing agent  $\text{SynAgent}_{m^*}$ .

First, we define the total number of correct responses provided by the  $m$ -th synthesis agent (which generates  $K$  CoTs for the  $n$ -th sample) as:

$$A_{n,m} = \sum_{k=1}^K \text{LLMJudge}(\hat{a}_{n,m,k}, a_n). \quad (8)$$

This metric reflects the agent’s ability to produce correct answers, i.e., among the  $K$  responses, how many match the reference answer. This corresponds to *Answer Correctness*.

Next, we define the total number of valid CoTs synthesized by the same agent as:

$$V_{n,m} = \sum_{k=1}^K \text{LLMJudge}(v_{n,m,k}, a_n). \quad (9)$$

This metric reflects the reliability of the reasoning paths, which corresponds to *Reasoning Validity*.

Finally, we rank the  $m$  agents based on their  $V_{n,m}$  scores. If two or more agents exhibit comparable reliability (i.e., similar  $V_{n,m}$ ), we break the tie by further ranking them based on their answer correctness  $A_{n,m}$ .

After determining the *synthesis agent*, in CoT Selection, we first discard all CoTs generated by the selected agent with incorrect answers (i.e.,  $\text{LLMJudge}(\hat{a}, a) = 0$ ). Next, we employ both *Reasoning Validity* and *Length Appropriateness* to identify the highest-scoring CoT based on:

$$k^* = \arg \max_k (\phi(v_{n, m^*, k}) + \lambda_k \cdot r_{n, m^*, k}), \quad (10)$$

where  $\phi(v_{n, m^*, k})$  is the confidence of the small model’s responses and  $r_{n, m^*, k}$  measures the length appropriateness.

As a result, for each instance  $q_n$ , we can obtain its corresponding optimal reasoning trajectory  $\text{CoT}_{n, m^*, k^*}$ , thereby constructing the multimodal reasoning dataset  $\mathcal{D}_{\text{cot}}$ .

### 4.3. Batch Selection

Appropriate SFT data can play a crucial role in the early stages of MLRMs training. It helps guide the model toward learning correct reasoning patterns and facilitates more significant performance gains after RL post-training. However, this guiding effect depends more on quality than quantity. Therefore, at this stage, given the full dataset  $\mathcal{D}_{\text{cot}}$ , we aim to select the most instructive  $N'$  samples out of the total  $N$  instances, which are most helpful for fostering reasoning capabilities in the model. Since each instance in our generated dataset consists of a query and a corresponding CoT, we perform batch selection from both the query perspective and the CoT perspective with the LLMPlayer in *Reasoning Validity*.

#### 4.3.1. Query-aware Selection

To identify training samples that effectively improve reasoning ability, we first focus on queries whose predictions are significantly influenced by the presence of CoT. Intuitively, if a query leads to incorrect predictions without CoT but is answered correctly with CoT, it suggests that the query is non-trivial and that the CoT provides meaningful guidance. Such queries are more valuable for training, as they highlight reasoning challenges that benefit from exemplified thought processes.

Specifically, for each query  $q_n$ , we first evaluate the performance of the LLMPlayer without any CoT assistance. To ensure consistency with the CoT-aided setting, we perform  $M \times K$  inference rounds using different sampling seeds:

$$\tilde{v}_{n,m,k} = \text{LLMPlayer}(q_n; \varepsilon_{n,m,k}). \quad (11)$$

We then compare the LLMPlayer’s performance with and without CoT by computing the number of correct re-

sponses in each query. Specifically, for the CoT-free setting:

$$\tilde{v}_{n,m,k} = \text{LLMPlayer}(q_n; \varepsilon_{n,m,k}). \quad (12)$$

For the CoT-aided setting:

$$\alpha_n = \sum_{m,k} \text{LLMJudge}(v_{n,m,k}, a_n). \quad (13)$$

The accuracy gain brought by CoT is defined as:  $\Delta_\alpha = \alpha_n - \tilde{\alpha}_n$ , which serves as a proxy for the training value of query  $q_n$ . A larger gain indicates that the query benefits more from reasoning guidance and is therefore more informative for improving the model’s reasoning capabilities.

However, the accuracy gain has a limitation: It does not fully capture the inherent difficulty of each query. For example, suppose  $M = 3$  and  $K = 6$ , resulting in 18 CoTs per query. Consider two queries with the same accuracy gain  $\alpha_n - \tilde{\alpha}_n$ :  $12 - 10$  and  $5 - 3$ . Although both exhibit a gain of 2, the latter is clearly more challenging. Such query are arguably more valuable for fostering the model’s complex reasoning ability. To better reflect this aspect, we further introduce the CoT-aware selection.

#### 4.3.2. CoT-aware Selection

Given the generated dataset  $\mathcal{D}_{\text{cot}}$ , each query is associated with a best-performing CoT. If the model exhibits higher confidence when responding with it compared to without any CoT, this implies a stronger belief in its reasoning process, which is desirable for effective learning. Therefore, we define the following indicators based on Eq(6):

$$\begin{aligned} \beta_n^* &= \phi(v_{n, m^*, k^*}), \quad \tilde{\beta}_{n,m,k} = \phi(\tilde{v}_{n,m,k}), \\ \Delta_\beta &= \beta_n^* - \frac{1}{MK} \sum_{m,k} \tilde{\beta}_{n,m,k}, \end{aligned} \quad (14)$$

where  $\beta_n^*$  denotes the confidence of the model’s best CoT-aided prediction, while the second term is the average confidence over all non-CoT predictions. The difference  $\Delta_\beta$  captures the confidence gain provided by the CoT. A higher  $\Delta_\beta$  indicates that the CoT significantly boosts the model’s belief in its answer, highlighting the CoT’s effectiveness in guiding the reasoning process.

Besides, we further introduce a correctness reward, defined as  $f(v, a) = 2 \cdot \text{LLMJudge}(v, a) - 1$ . This is a constant term that takes the value of +1 when the model prediction  $v$  matches the correct answer  $a$ , and  $-1$  otherwise, since  $\text{LLMJudge}(v, a)$  equals 1 for correct predictions and 0 for incorrect ones (i.e., Eq(4)). Then, the final reward score is defined as:

$$\begin{aligned} \gamma_n^* &= f(v_{n, m^*, k^*}, a_n), \quad \tilde{\gamma}_{n,m,k} = f(\tilde{v}_{n,m,k}, a_n), \\ \Delta_\gamma &= \gamma_n^* - \frac{1}{MK} \sum_{m,k} \tilde{\gamma}_{n,m,k}. \end{aligned} \quad (15)$$

This score ensures that LLMPlayer receives higher rewards only when it correctly answers queries, thus making the selection process more meaningful.

Model	MathVerse-ALL	MathVerse-Vision Only	MathVista	WeMath
<b>Base Model</b>				
Qwen2.5-VL-7B	43.6	38.2	63.7	61.0
<b>Other Models</b>				
GPT-4o	41.2	34.5	60.0	69.0
InternVL2.5-8B	35.6	22.8	64.5	53.8
Qwen2-VL-7B	30.2	25.4	61.6	50.5
LLaVA-CoT-11B	-	22.6	52.5	-
<b>SFT Only</b>				
R1-Onevision(rpt)	43.4	39.7	-	-
R1-Onevision	41.9±0.6	38.0±0.9	59.9±2.3	57.6±0.6
SynSelect- $\mathcal{D}'_{cot}$	44.2±0.7	40.2±0.7	63.1±1.9	60.2±1.3
SynSelect- $\mathcal{D}'_{cot}$	<b>45.2±0.7</b>	<b>41.7±1.0</b>	<b>64.3±0.8</b>	<b>61.8±0.6</b>
<b>RL Only</b>				
Qwen2.5-VL-7B	43.9±0.8	39.2±0.7	62.8±1.4	59.1±1.1
<b>SFT + RL</b>				
R1-Onevision(rpt)	<b>46.4</b>	40.0	64.1	61.8
R1-Onevision	44.6±0.3	40.0±0.8	64.2±0.6	59.0±0.7
SynSelect- $\mathcal{D}'_{cot}$	45.0±0.4	40.3±0.5	<b>66.0±1.4</b>	61.2±0.9
SynSelect- $\mathcal{D}'_{cot}$	46.1±0.3	<b>41.9±1.1</b>	65.7±1.2	<b>62.8±1.4</b>

Table 1. Experimental results on multimodal reasoning benchmarks. Except for models trained on the R1-Onevision-Dataset and SynSelect data, all results are taken from the original R1-Onevision paper, with ‘‘R1-Onevision (rpt)’’ indicates the reported values. Reproduced experiments are reported as (mean±std). The highest accuracy in each group is highlighted in **bold**.

To further illustrate the effect of the correctness reward, consider the same example used in Query-aware Selection, where two queries share the same accuracy gain. We first suppose the best CoT in both cases yields a correct answer, i.e.,  $\gamma_n^* = 1$ . Then, for the first query where  $\tilde{\alpha}_n = 10$  (10 correct, 8 incorrect among 18 CoTs), we have:  $\Delta_\gamma = 1 - \frac{1}{18}(10 - 8) = \frac{8}{9}$ . Similarly, for the second query with  $\tilde{\alpha}_n = 3$  (3 correct, 15 incorrect), we get:  $\Delta_\gamma = 1 - \frac{1}{18}(3 - 15) = \frac{5}{3}$ . Although both queries have the same accuracy gain, the latter receives a higher reward due to its higher difficulty, making it more likely to be selected for training.

Finally, combining the query-aware and the CoT-aware selection, we define the final selection score as:

$$S(n) = \lambda_\alpha \Delta_\alpha + \lambda_\beta \Delta_\beta + \lambda_\gamma \Delta_\gamma. \quad (16)$$

Using the above formula, we can compute a selection score for each instance in the dataset  $\mathcal{D}_{cot}$ . We then rank all  $N$  instances by their scores and select the top  $N'$  instances to construct the refined dataset  $\mathcal{D}'_{cot}$ .

## 5. Experiments

### 5.1. Experiment Settings

**Dataset and Benchmarks.** We conduct experiments on the R1-Onevision-Dataset [40], a multimodal dataset containing 154,667 image-question-answer (IQA) instances, each paired with a CoT reasoning path that is synthesized with the vision-to-text conversion method. To construct our raw multimodal dataset  $\mathcal{D}_{raw}$ , we remove the original CoTs and retain only the IQA pairs. After building  $\mathcal{D}_{cot}$  and  $\mathcal{D}'_{cot}$ , for fair comparison, we follow the same training pipeline as R1-Onevision, including SFT followed by

RL optimization, to obtain MLRMs. Throughout all experiments, we use Qwen2.5-VL-7B [1] as the model backbone. In the evaluation phase, we assess performance on several mainstream multimodal reasoning benchmarks, including MathVerse [48], MathVista [19], WeMath [24], and R1-Onevision-Bench [40], using accuracy as the evaluation metric. Detailed descriptions of the datasets are provided in the Appendix.

**Comparison Methods.** We compare our proposed method with the following models: (1) the baseline R1-Onevision model [40]; (2) the base model Qwen2.5-VL-7B[1]; and (3) several representative state-of-the-art (SoTA) models, including GPT-4o [12], InternVL2.5-8B [5], Qwen2-VL-7B [32], and LLaVA-CoT-11B [38]. Among them, LLaVA-CoT-11B employs a four-stage CoT synthesis enhance its reasoning capabilities.

**Implementation Details.** The Qwen2.5-VL series is employed as baseline models. For LLM Extractors, we use Qwen3-8B [39]. In experiments, we take  $M = 3$ ,  $K = 6$ . The SynAgents are R1-Onevision [40], MM-Eureka [21], and Vision-R1 [11], respectively. For the score coefficients, we adopt  $\lambda_k = 1$ ,  $\lambda_\alpha = 2$ ,  $\lambda_\beta = 1$ ,  $\lambda_\gamma = 1$ . During RL training (i.e., GRPO [27]), we employ CLEVR [13] as our training dataset. Moreover, for evaluations, we conducted five independent runs. Further details regarding dataset construction, training procedures, and benchmark specifications are available in the Appendix.

### 5.2. Main Results

**Model Performance.** We first fine-tune MLLMs with CoT data synthesized by SynSelect, followed by RL optimization (GRPO). As shown in Table 1, models trained on both

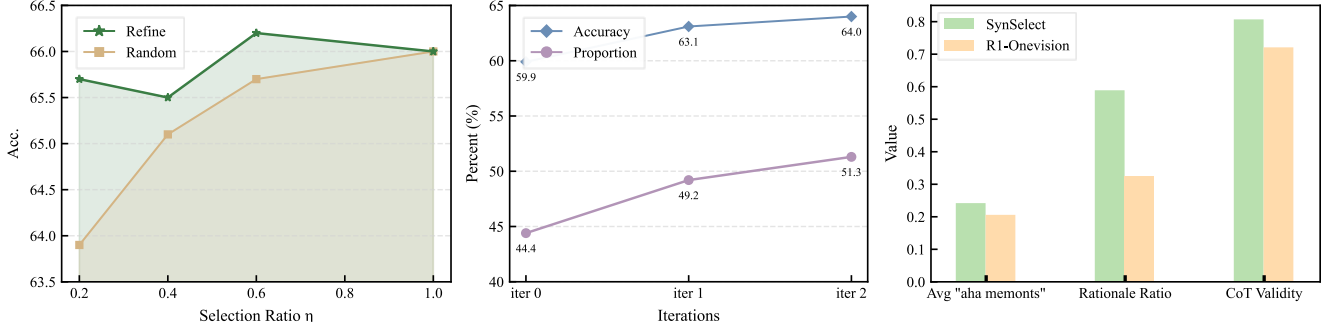


Figure 4. **(Left)** Sensitivity analysis of the selection ratio  $\eta$ . Experiments are conducted on the MathVista benchmark. **(Middle)** Results of the iterative bootstrap experiment. Evaluations are conducted on MathVista. **(Right)** Quantitative analysis of data quality. In addition to the Rationale Ratio defined in Section 4.2, we also report the Avg “aha moments” and CoT Validity, as introduced in Section 5.2.

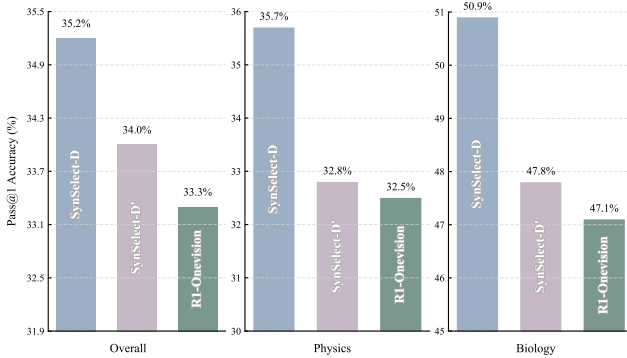


Figure 5. Experimental results on R1-Onevision-Bench.

$\mathcal{D}_{\text{cot}}$  and  $\mathcal{D}'_{\text{cot}}$  consistently outperform existing SoTA methods across most multimodal reasoning benchmarks. Notably, SynSelect- $\mathcal{D}_{\text{cot}}$  achieves around 2% gains over R1-Onevision on MathVista and WeMath, and even surpasses LLaVA-CoT-11B, demonstrating that the proposed CoT synthesis strategy is more effective than existing CoT construction methods for enhancing multimodal reasoning performance. Moreover,  $\mathcal{D}'_{\text{cot}}$  further improves performance, showing that a compact subset of high-quality CoTs can better enhance complex reasoning ability and training efficiency.

We further evaluate SynSelect on R1-Onevision-Bench, a multimodal reasoning benchmark covering a variety of domains such as physics, biology, and related areas. All models are trained under the same SFT+RL setup for fair comparison. As shown in Figure 5, models trained on SynSelect-synthesized data consistently outperform those trained on the original R1-Onevision dataset across all domains, confirming that SynSelect-generated CoTs generalize effectively to diverse reasoning scenarios. Interestingly, unlike our earlier results on mathematical reasoning benchmarks, the full dataset  $\mathcal{D}_{\text{cot}}$  yields the best performance on R1-Onevision-Bench. A plausible explanation is that

larger-scale SFT data provides a wider exploration space, enabling the model to handle heterogeneous problem types more effectively.

**Data Quality.** Beyond performance, we assess the synthesized data from multiple perspectives, including “aha moments”, rationale ratio, and CoT validity. As shown in Figure 4 (right), Avg “aha moments” indicates the average occurrence frequency of trigger tokens (i.e., “Wait...”) in the data. Rationale ratio has been presented in Section 4.2. CoT Validity refers to the accuracy of LLMPlayer in answering questions when the corresponding CoT is provided as input. Compared with R1-Onevision, SynSelect yields clear improvements across all metrics, especially in rationale ratio, indicating that it constructs more coherent and informative reasoning chains.

**Analysis of Selection Mechanism.** In this section, we investigate the effect of the selection ratio  $\eta$  by setting  $\eta = \{0.2, 0.4, 0.6, 1.0\}$ . As shown in Figure 4 (left), models trained on the refined subset  $\mathcal{D}'_{\text{cot}}$  consistently outperform randomly sampled data. Notably, when the sampling rate is 20%, the performance of randomly sampled data drops significantly. Moreover, 20% of selected data matches or exceeds the performance of 60% of random data. These results clearly demonstrate that the quality of SFT data is critical for improving a model’s reasoning ability, and that an effective selection mechanism is essential for maximizing training efficiency and performance.

### 5.3. Ablation Study

In addition to evaluating models trained with SFT+RL, we also assess the performance of models trained with SFT alone. As shown in Table 1, models trained on SynSelect-synthesized data without RL consistently outperform those trained on the original R1-Onevision dataset. On both MathVista and WeMath, our method achieves approximately a 4% improvement over the baseline, further demonstrating the effectiveness of the proposed CoT synthesis approach.

Model	MathVerse ALL	MathVerse Vision-only	MathVista
<i>Base Model</i>			
Qwen2.5-VL	43.6	38.2	63.7
<i>SFT Only</i>			
Qwen2.5-VL	43.1±1.0	38.5±0.9	64.5±1.5
<i>SynSelect-D<sub>cot</sub></i>	<b>43.7±0.2</b>	39.1±0.7	<b>65.6±1.6</b>
<i>SynSelect-D'<sub>cot</sub></i>	43.4±0.3	<b>39.5±0.9</b>	64.7±1.4
<i>SFT + RL</i>			
Qwen2.5-VL	44.2±1.3	39.7±1.6	66.8±1.8
<i>SynSelect-D<sub>cot</sub></i>	45.7±2.2	40.9±2.1	66.3±1.0
<i>SynSelect-D'<sub>cot</sub></i>	<b>46.9±1.5</b>	<b>42.4±2.4</b>	<b>67.1±2.6</b>

Table 2. Experimental results on multimodal reasoning benchmarks. Unlike Table 1, we have changed the raw dataset and taken Vision-R1-Cold as  $\mathcal{D}_{\text{raw}}$ . Results are reported as (mean±std). The highest accuracy in each group is highlighted in **bold**.

## 5.4. Scalability

To assess the scalability of *SynSelect*, we further replace the original raw dataset  $\mathcal{D}_{\text{raw}}$  with Vision-R1-Cold [11], which differs from R1-OneVision-Dataset in data distribution and modality conversion strategy. This experiment examines whether *SynSelect* generalizes to new data sources. As shown in Table 2, *SynSelect* consistently improves performance across all benchmarks under this new setting. Both *SynSelect-D<sub>cot</sub>* and *SynSelect-D'<sub>cot</sub>* outperform the Qwen2.5-VL baseline in SFT-only and SFT+RL stages, achieving the highest accuracies on MathVerse and MathVista. These results confirm that *SynSelect*’s synthesis–selection mechanism generalizes well across datasets, demonstrating strong scalability and robustness in multimodal reasoning tasks.

## 5.5. Iterative Bootstrap

We further explore whether *SynSelect* can self-improve through iterative refinement. Starting from a model fine-tuned on R1-OneVision-Dataset, we repeatedly use it as SynAgent to synthesize new CoT data, fine-tune the base model, and replace the SynAgent in a closed loop of “generate → fine-tune → regenerate.”

As shown in Figure 4 (middle), both reasoning accuracy and the proportion of self-generated data increase consistently across iterations—from 59.9% to 64.0% and 44.4% to 51.3%, respectively. This trend reveals a positive feedback loop between model improvement and data quality, demonstrating that *SynSelect* acts as a self-bootstrapping data engine capable of continual autonomous enhancement.

## 6. Conclusion

In this paper, we proposed *SynSelect*, a three-stage synthesis–selection framework for constructing high-quality long CoT data tailored to multimodal reasoning tasks. Specifically, *SynSelect* first synthesized comprehensive and

diverse reasoning paths by leveraging multiple heterogeneous MLRMs. Then, we employed an instance-level selection strategy to identify the most suitable CoT for each instance based on answer correctness, reasoning validity, and length appropriateness metrics. Finally, we selected a compact and instructive subset through batch selection strategies, including query-aware and CoT-aware selection methods. Experimental results on multiple multimodal benchmarks demonstrated the effectiveness of our framework.

## References

- [1] Shuai Bai, Keqin Chen, Xuejing Liu, Jialin Wang, Wenbin Ge, Sibao Song, Kai Dang, Peng Wang, Shijie Wang, Jun Tang, Humen Zhong, Yuanzhi Zhu, Mingkun Yang, Zhaohai Li, Jianqiang Wan, Pengfei Wang, Wei Ding, Zheren Fu, Yiheng Xu, Jiabo Ye, Xi Zhang, Tianbao Xie, Zesen Cheng, Hang Zhang, Zhibo Yang, Haiyang Xu, and Junyang Lin. Qwen2.5-VL Technical Report, 2025. arXiv:2502.13923 [cs]. 3, 5, 7
- [2] Hardy Chen, Haoqin Tu, Fali Wang, Hui Liu, Xianfeng Tang, Xinya Du, Yuyin Zhou, and Cihang Xie. Sft or rl? an early investigation into training rl-like reasoning large vision-language models. *arXiv preprint arXiv:2504.11468*, 2025. 3
- [3] Liang Chen, Hongcheng Gao, Tianyu Liu, Zhiqi Huang, Flood Sung, Xinyu Zhou, Yuxin Wu, and Baobao Chang. G1: Bootstrapping perception and reasoning abilities of vision-language model via reinforcement learning. *arXiv preprint arXiv:2505.13426*, 2025. 2, 3
- [4] Shuang Chen, Yue Guo, Zhaochen Su, Yafu Li, Yulun Wu, Jiacheng Chen, Jiayu Chen, Weijie Wang, Xiaoye Qu, and Yu Cheng. Advancing multimodal reasoning: From optimized cold start to staged reinforcement learning. *arXiv preprint arXiv:2506.04207*, 2025. 2, 3
- [5] Zhe Chen, Weiyun Wang, Yue Cao, Yangzhou Liu, Zhangwei Gao, Erfei Cui, Jinguo Zhu, Shenglong Ye, Hao Tian, Zhaoyang Liu, et al. Expanding performance boundaries of open-source multimodal models with model, data, and test-time scaling. *arXiv preprint arXiv:2412.05271*, 2024. 3, 7
- [6] DeepSeek-AI, Daya Guo, Dejian Yang, Haowei Zhang, Junxiao Song, Ruoyu Zhang, Runxin Xu, Qihao Zhu, Shitong Ma, and Peiyi et al. Wang. DeepSeek-R1: Incentivizing Reasoning Capability in LLMs via Reinforcement Learning, 2025. arXiv:2501.12948 [cs]. 2, 1
- [7] DeepSeek-AI, Aixin Liu, Bei Feng, Bing Xue, Bingxuan Wang, Bochao Wu, Chengda Lu, Chenggang Zhao, Chengqi Deng, and Chenyu et al. Zhang. DeepSeek-V3 Technical Report, 2025. arXiv:2412.19437 [cs]. 2
- [8] Yihe Deng, Hritik Bansal, Fan Yin, Nanyun Peng, Wei Wang, and Kai-Wei Chang. Openvlthinker: An early exploration to complex vision-language reasoning via iterative self-improvement. *arXiv preprint arXiv:2503.17352*, 2025. 3
- [9] Abhimanyu Dubey, Abhinav Jauhri, Abhinav Pandey, Abhishek Kadian, Ahmad Al-Dahle, Aiesha Letman, Akhil Mathur, Alan Schelten, Amy Yang, and Angela Fan. The

- llama 3 herd of models. *arXiv e-prints*, pages arXiv-2407, 2024. 3
- [10] Dan Hendrycks, Collin Burns, Steven Basart, Andy Zou, Mantas Mazeika, Dawn Song, and Jacob Steinhardt. Measuring massive multitask language understanding. *arXiv preprint arXiv:2009.03300*, 2020. 2
- [11] Wenxuan Huang, Bohan Jia, Zijie Zhai, Shaosheng Cao, Zheyu Ye, Fei Zhao, Zhe Xu, Yao Hu, and Shaohui Lin. Vision-r1: Incentivizing reasoning capability in multimodal large language models. *arXiv preprint arXiv:2503.06749*, 2025. 2, 3, 4, 7, 9, 1
- [12] Aaron Hurst, Adam Lerer, Adam P Goucher, Adam Perelman, Aditya Ramesh, Aidan Clark, AJ Ostrow, Akila Welihinda, Alan Hayes, Alec Radford, et al. Gpt-4o system card. *arXiv preprint arXiv:2410.21276*, 2024. 3, 7
- [13] Justin Johnson, Bharath Hariharan, Laurens Van Der Maaten, Li Fei-Fei, C Lawrence Zitnick, and Ross Girshick. Clevr: A diagnostic dataset for compositional language and elementary visual reasoning. In *Proceedings of the IEEE conference on computer vision and pattern recognition*, pages 2901–2910, 2017. 7
- [14] KimiTeam, Angang Du, Bohong Yin, Bowei Xing, Bowen Qu, Bowen Wang, Cheng Chen, Chenlin Zhang, Chen-zhuang Du, and Chu et al. Wei. Kimi-VL Technical Report, 2025. arXiv:2504.07491 [cs]. 3
- [15] Bo Li, Yuanhan Zhang, Dong Guo, Renrui Zhang, Feng Li, Hao Zhang, Kaichen Zhang, Peiyuan Zhang, Yanwei Li, Ziwei Liu, and Chunyuan Li. LLaVA-OneVision: Easy Visual Task Transfer, 2024. arXiv:2408.03326 [cs]. 3
- [16] Zhong-Zhi Li, Duzhen Zhang, Ming-Liang Zhang, Jiaxin Zhang, Zengyan Liu, Yuxuan Yao, Haotian Xu, Junhao Zheng, Pei-Jie Wang, Xiuyi Chen, Yingying Zhang, Fei Yin, Jiahua Dong, Zhiwei Li, Bao-Long Bi, Ling-Rui Mei, Junfeng Fang, Xiao Liang, Zhijiang Guo, Le Song, and Cheng-Lin Liu. From System 1 to System 2: A Survey of Reasoning Large Language Models, 2025. arXiv:2502.17419 [cs]. 2
- [17] Yuan Liu, Haodong Duan, Yuanhan Zhang, Bo Li, Songyang Zhang, Wangbo Zhao, Yike Yuan, Jiaqi Wang, Conghui He, Ziwei Liu, et al. Mmbench: Is your multi-modal model an all-around player? In *European conference on computer vision*, pages 216–233. Springer, 2024. 2, 3
- [18] Pan Lu, Swaroop Mishra, Tanglin Xia, Liang Qiu, Kai-Wei Chang, Song-Chun Zhu, Oyvind Taffjord, Peter Clark, and Ashwin Kalyan. Learn to explain: Multimodal reasoning via thought chains for science question answering. *Advances in Neural Information Processing Systems*, 35:2507–2521, 2022. 2, 3
- [19] Pan Lu, Hritik Bansal, Tony Xia, Jiacheng Liu, Chunyuan Li, Hannaneh Hajishirzi, Hao Cheng, Kai-Wei Chang, Michel Galley, and Jianfeng Gao. Mathvista: Evaluating mathematical reasoning of foundation models in visual contexts. *arXiv preprint arXiv:2310.02255*, 2023. 7, 1
- [20] Ahmed Masry, Do Xuan Long, Jia Qing Tan, Shafiq Joty, and Enamul Hoque. Chartqa: A benchmark for question answering about charts with visual and logical reasoning. *arXiv preprint arXiv:2203.10244*, 2022. 3
- [21] Fanqing Meng, Lingxiao Du, Zongkai Liu, Zhixiang Zhou, Quanfeng Lu, Daocheng Fu, Botian Shi, Wenhai Wang, Junjun He, Kaipeng Zhang, et al. Mm-eureka: Exploring visual aha moment with rule-based large-scale reinforcement learning. *CoRR*, 2025. 2, 3, 4, 7, 1
- [22] OpenAI, Aaron Jaech, Adam Kalai, Adam Lerer, Adam Richardson, Ahmed El-Kishky, Aiden Low, Alec Helyar, and Aleksander et al. Madry. OpenAI o1 System Card, 2024. arXiv:2412.16720 [cs]. 2
- [23] Yingzhe Peng, Gongrui Zhang, Miaosen Zhang, Zhiyuan You, Jie Liu, Qipeng Zhu, Kai Yang, Xingzhong Xu, Xin Geng, and Xu Yang. Lmm-r1: Empowering 3b lms with strong reasoning abilities through two-stage rule-based rl. *arXiv preprint arXiv:2503.07536*, 2025. 2, 3
- [24] Runqi Qiao, Qiuna Tan, Guanting Dong, Minhui Wu, Chong Sun, Xiaoshuai Song, Zhuoma GongQue, Shanglin Lei, Zhe Wei, Miaoxuan Zhang, et al. We-math: Does your large multimodal model achieve human-like mathematical reasoning? *arXiv preprint arXiv:2407.01284*, 2024. 7, 1
- [25] QwenTeam. Qvq: To see the world with wisdom, 2024. 3
- [26] QwenTeam. Qwq: Reflect deeply on the boundaries of the unknown, 2024. 2
- [27] Zhihong Shao, Peiyi Wang, Qihao Zhu, Runxin Xu, Junxiao Song, Xiao Bi, Haowei Zhang, Mingchuan Zhang, YK Li, Yang Wu, et al. Deepseekmath: Pushing the limits of mathematical reasoning in open language models. *arXiv preprint arXiv:2402.03300*, 2024. 4, 7
- [28] Haozhan Shen, Peng Liu, Jingcheng Li, Chunxin Fang, Yibo Ma, Jiajia Liao, Qiaoli Shen, Zilun Zhang, Kangjia Zhao, Qianqian Zhang, et al. Vlm-r1: A stable and generalizable r1-style large vision-language model. *arXiv preprint arXiv:2504.07615*, 2025. 3
- [29] StepFunTeam. Step3: Cost-effective multimodal intelligence. 3
- [30] Huajie Tan, Yuheng Ji, Xiaoshuai Hao, Minglan Lin, Pengwei Wang, Zhongyuan Wang, and Shanghang Zhang. Reason-rft: Reinforcement fine-tuning for visual reasoning. *arXiv preprint arXiv:2503.20752*, 2025. 3
- [31] Omkar Thawakar, Dinura Dissanayake, Ketan More, Ritesh Thawkar, Ahmed Heakl, Noor Ahsan, Yuhao Li, Mohammed Zumri, Jean Lahoud, Rao Muhammad Anwer, Hisham Cholakkal, Ivan Laptev, Mubarak Shah, Fahad Shahbaz Khan, and Salman Khan. LlamaV-o1: Rethinking Step-by-step Visual Reasoning in LLMs, 2025. arXiv:2501.06186 [cs]. 3
- [32] Peng Wang, Shuai Bai, Sinan Tan, Shijie Wang, Zhihao Fan, Jinze Bai, Keqin Chen, Xuejing Liu, Jialin Wang, and Wenbin et al. Ge. Qwen2-vl: Enhancing vision-language model’s perception of the world at any resolution. *arXiv preprint arXiv:2409.12191*, 2024. 3, 7
- [33] Peiyu Wang, Yichen Wei, Yi Peng, Xiaokun Wang, Weijie Qiu, Wei Shen, Tianyidan Xie, Jiangbo Pei, Jianhao Zhang, Yunzhuo Hao, et al. Skywork r1v2: Multimodal hybrid reinforcement learning for reasoning. *arXiv preprint arXiv:2504.16656*, 2025. 3
- [34] Weiyun Wang, Zhe Chen, Wenhai Wang, Yue Cao, Yangzhou Liu, Zhangwei Gao, Jinguo Zhu, Xizhou Zhu, Lewei Lu, Yu Qiao, et al. Enhancing the reasoning ability of multimodal large language models via mixed preference optimization. *arXiv preprint arXiv:2411.10442*, 2024. 3

- [35] Weiyun Wang, Zhe Chen, Wenhai Wang, Yue Cao, Yangzhou Liu, Zhangwei Gao, Jinguo Zhu, Xizhou Zhu, Lewei Lu, Yu Qiao, and Jifeng Dai. Enhancing the Reasoning Ability of Multimodal Large Language Models via Mixed Preference Optimization, 2025. [arXiv:2411.10442 \[cs\]](#). 3
- [36] Zhiyu Wu, Xiaokang Chen, Zizheng Pan, Xingchao Liu, Wen Liu, Damai Dai, Huazuo Gao, Yiyang Ma, Chengyue Wu, Bingxuan Wang, Zhenda Xie, Yu Wu, Kai Hu, Jiawei Wang, Yaofeng Sun, Yukun Li, Yishi Piao, Kang Guan, Aixin Liu, Xin Xie, Yuxiang You, Kai Dong, Xingkai Yu, Haowei Zhang, Liang Zhao, Yisong Wang, and Chong Ruan. DeepSeek-VL2: Mixture-of-Experts Vision-Language Models for Advanced Multimodal Understanding, 2024. [arXiv:2412.10302 \[cs\]](#). 3
- [37] Tian Xie, Zitian Gao, Qingnan Ren, Haoming Luo, Yuqian Hong, Bryan Dai, Joey Zhou, Kai Qiu, Zhirong Wu, and Chong Luo. Logic-RL: Unleashing LLM Reasoning with Rule-Based Reinforcement Learning, 2025. [arXiv:2502.14768 \[cs\]](#). 2
- [38] Guowei Xu, Peng Jin, Ziang Wu, Hao Li, Yibing Song, Lichao Sun, and Li Yuan. LLaVA-CoT: Let Vision Language Models Reason Step-by-Step, 2025. [arXiv:2411.10440 \[cs\]](#). 2, 3, 7
- [39] An Yang, Anfeng Li, Baosong Yang, Beichen Zhang, Binyuan Hui, Bo Zheng, Bowen Yu, Chang Gao, Chengen Huang, Chenxu Lv, et al. Qwen3 technical report. *arXiv preprint arXiv:2505.09388*, 2025. 2, 7
- [40] Yi Yang, Xiaoxuan He, Hongkun Pan, Xiyan Jiang, Yan Deng, Xingtao Yang, Haoyu Lu, Dacheng Yin, Fengyun Rao, Minfeng Zhu, et al. R1-onevision: Advancing generalized multimodal reasoning through cross-modal formalization. *arXiv preprint arXiv:2503.10615*, 2025. 2, 3, 4, 7, 1
- [41] Huanjin Yao, Jiaying Huang, Wenhao Wu, Jingyi Zhang, Yibo Wang, Shunyu Liu, Yingjie Wang, Yuxin Song, Haocheng Feng, Li Shen, and Dacheng Tao. Mulberry: Empowering MLLM with o1-like Reasoning and Reflection via Collective Monte Carlo Tree Search, 2024. [arXiv:2412.18319 \[cs\]](#). 3
- [42] Huanjin Yao, Jiaying Huang, Wenhao Wu, Jingyi Zhang, Yibo Wang, Shunyu Liu, Yingjie Wang, Yuxin Song, Haocheng Feng, Li Shen, et al. Mulberry: Empowering mllm with o1-like reasoning and reflection via collective monte carlo tree search. *arXiv preprint arXiv:2412.18319*, 2024. 3
- [43] Yuan Yao, Tianyu Yu, Ao Zhang, Chongyi Wang, Junbo Cui, Hongji Zhu, Tianchi Cai, Haoyu Li, Weilin Zhao, Zhihui He, Qianyu Chen, Huarong Zhou, Zhensheng Zou, Haoye Zhang, Shengding Hu, Zhi Zheng, Jie Zhou, Jie Cai, Xu Han, Guoyang Zeng, Dahai Li, Zhiyuan Liu, and Maosong Sun. MiniCPM-V: A GPT-4V Level MLLM on Your Phone, 2024. [arXiv:2408.01800 \[cs\]](#). 3
- [44] Shukang Yin, Chaoyou Fu, Sirui Zhao, Ke Li, Xing Sun, Tong Xu, and Enhong Chen. A survey on multimodal large language models. *National Science Review*, 11(12), 2024. 2
- [45] Duzhen Zhang, Yahan Yu, Jiahua Dong, Chenxing Li, Dan Su, Chenhui Chu, and Dong Yu. Mm-llms: Recent advances in multimodal large language models. *arXiv preprint arXiv:2401.13601*, 2024. 2
- [46] Haotian Zhang, Mingfei Gao, Zhe Gan, Philipp Dufter, Nina Wenzel, Forrest Huang, Dhruvi Shah, Xianzhi Du, Bowen Zhang, Yanghao Li, Sam Dodge, Keen You, Zhen Yang, Aleksei Timofeev, Mingze Xu, Hong-You Chen, Jean-Philippe Fauconnier, Zhengfeng Lai, Haoxuan You, Zirui Wang, Afshin Dehghan, Peter Grasch, and Yinfei Yang. MM1.5: Methods, Analysis & Insights from Multimodal LLM Fine-tuning, 2024. [arXiv:2409.20566 \[cs\]](#). 3
- [47] Jingyi Zhang, Jiaying Huang, Huanjin Yao, Shunyu Liu, Xikun Zhang, Shijian Lu, and Dacheng Tao. R1-VL: Learning to Reason with Multimodal Large Language Models via Step-wise Group Relative Policy Optimization, 2025. [arXiv:2503.12937 \[cs\]](#). 3
- [48] Renrui Zhang, Dongzhi Jiang, Yichi Zhang, Haokun Lin, Ziyu Guo, Pengshuo Qiu, Aojun Zhou, Pan Lu, Kai-Wei Chang, Yu Qiao, et al. Mathverse: Does your multi-modal llm truly see the diagrams in visual math problems? In *European Conference on Computer Vision*, pages 169–186. Springer, 2024. 7, 1
- [49] Hengguang Zhou, Xirui Li, Ruochen Wang, Minhao Cheng, Tianyi Zhou, and Cho-Jui Hsieh. R1-zero’s” aha moment” in visual reasoning on a 2b non-sft model. *arXiv preprint arXiv:2503.05132*, 2025. 3



# Training Multimodal Large Reasoning Models Needs Better Thoughts: A Three-Stage Framework for Long Chain-of-Thought Synthesis and Selection

## Supplementary Material

### 1. Details of Dataset and Benchmarks

Our framework is built upon the R1-Onevision-Dataset [40], and the trained models are evaluated across multiple multimodal reasoning benchmarks, including MathVista [19], MathVerse [48], and WeMath [24]:

**Dataset** R1-Onevision-Dataset [40] is a multimodal reasoning dataset that includes samples from domains such as science, mathematics, charts, and natural scenarios, with a total of over 155k examples. Each sample contains an image-question-answer (IQA) pair along with a Chain-of-Thought (CoT). The original CoTs were generated using a text-based reasoning model (e.g., DeepSeek-R1 [6]) through an image-to-text conversion method. In this work, we remove the original CoTs and regenerate them using the *SynSelect* framework.

#### Benchmarks

- MathVista [19]: a mathematical benchmark constructed to integrate challenges across diverse mathematical and visual tasks. Its Test Mini split, containing approximately 1,000 samples, is utilized in our evaluation.
- MathVerse [48]: a comprehensive visual mathematics benchmark developed for equitable and in-depth assessment of multimodal large language models (MLLMs). We utilize the full dataset and additionally report the “Vision-Only” results, which expose substantial challenges by incorporating the entire question within the diagram.
- WeMath [24]: a benchmark designed to explore problem-solving mechanisms beyond end-to-end performance. We adopt its Test Mini split, comprising around 1,740 samples, with average accuracy serving as our primary reporting metric.
- R1-Onevision-Bench [40]: a comprehensive multimodal reasoning benchmark covering mathematics, physics, chemistry, biology, and logical deduction across 38 sub-categories. It comprises 942 problems paired with images. We adopt the full benchmark and report average accuracy as the primary metric.

### 2. Data Analysis

In this section, we present the basic statistics of the *SynSelect* dataset.

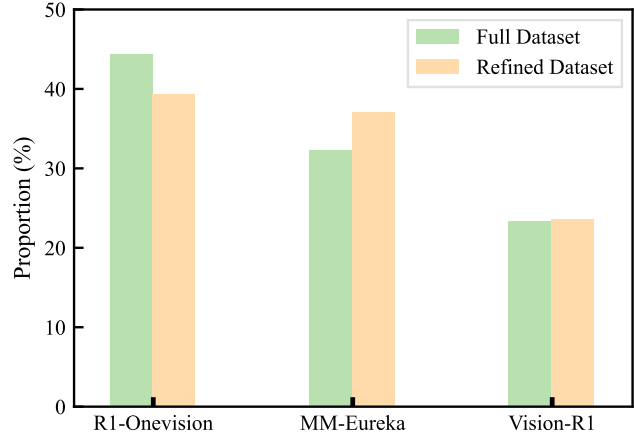


Figure 1. Source Distribution of Synthesized CoTs

The full synthesized dataset  $\mathcal{D}_{\text{cot}}$  consists of 150,435 CoTs, with an average length of 226.4 tokens and a standard deviation of 176.9. Among them, 66,864 CoTs are generated by R1-Onevision [40], while MM-Eureka [21] and Vision-R1 [11] contribute 48,522 and 35,044 samples, respectively.

The refined dataset  $\mathcal{D}'_{\text{cot}}$  contains 30,087 CoTs, with an average length of 196.5 tokens and a standard deviation of 133.5. Within this subset, 11,838 CoTs are from R1-Onevision [40], while MM-Eureka [21] and Vision-R1 [11] contribute 11,175 and 7,074 CoTs, respectively.

Figure 1 illustrates the proportion of CoTs contributed by each SynAgent in both datasets. In the full dataset  $\mathcal{D}_{\text{cot}}$ , R1-Onevision accounts for a relatively larger share. However, after refinement, the contributions become more balanced across different models. This shift suggests that the *SynSelect* framework is effective in leveraging the strengths of multiple models, resulting in a higher-quality and more diverse reasoning dataset.

### 3. Illustration of the *SynSelect* Pipeline

To illustrate the computation process of the *SynSelect* framework, we provide a simplified example. For ease of explanation, in Figure 2, we assume that two SynAgents are used, each generating two candidate CoTs, i.e.,  $M = 2$  and  $K = 2$ .

As shown in Figure 2, in the *Reason Trajectory Synthesis* phase, we generate  $M \times K = 2 \times 2 = 4$  candidate CoTs for each query.

Next, during the **Instance-Level Selection** phase, we select the optimal CoT for each query, resulting in the synthesized reasoning dataset  $\mathcal{D}_{\text{cot}}$ .

Finally, in the **Batch Selection** phase, we rank all queries based on the weighted score  $\lambda_{\alpha}\Delta_{\alpha} + \lambda_{\beta}\Delta_{\beta} + \lambda_{\gamma}\Delta_{\gamma}$ , and select the top- $N'$  instances according to the selection ratio  $\eta$ , yielding the refined reasoning dataset  $\mathcal{D}'_{\text{cot}}$ .

## 4. Case Study

### 4.1. SynSelect Data

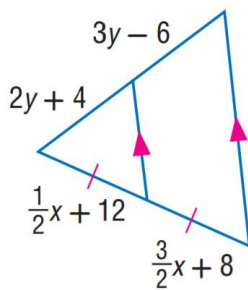
In this section, we present a case study on *SynSelect*-synthesized Data and compare them with the original CoTs in R1-Onevision-Dataset. Specific examples are provided in Figure 3-7.

### 4.2. Model Outputs

In this section, we present a case study on the performance of the model trained on *SynSelect*-synthesized data (SFT+RL), and compare it with the baseline R1-Onevision-7B-RL [40]. Specific examples are provided in Figure 8-12.

Reasoning Trajectory Synthesis														
$SynAgent_m$	$q_1$				$q_2$				$q_3$					
	$SynAgent_1$		$SynAgent_2$		$SynAgent_1$		$SynAgent_2$		$SynAgent_1$		$SynAgent_2$			
$CoT_{n,m,k}$	< think >	< think >	< think >	< think >	< think >	< think >	< think >	< think >	< think >	< think >	< think >	< think >	< think >	< think >
	⋮	⋮	⋮	⋮	⋮	⋮	⋮	⋮	⋮	⋮	⋮	⋮	⋮	⋮
	</think >	</think >	</think >	</think >	</think >	</think >	</think >	</think >	</think >	</think >	</think >	</think >	</think >	</think >
Instance-Level Selection														
$V_{n,m}$	2		1		1		1		0		1			
$A_{n,m}$	2		2		2		1		2		1			
$\hat{a}_{n,m,k}$	✓	✓	✓	✓	✓	✓	✓	×	✓	✓	✓	×		
$v_{n,m,k}$	✓	✓	✓	×	✓	×	✓	×	×	×	✓	×		
$r_{n,m,k}$	0.6	0.5	-	-	0.5	0.8	-	-	-	-	0.7	-		
$\phi(v_{n,m,k})$	0.3	0.5	-	-	0.4	0.3	-	-	-	-	0.3	-		
$r_{n,m,k} + \phi(v_{n,m,k})$	0.9	1.0	-	-	0.9	1.1	-	-	-	-	1.0	-		
$n^*, m^*, k^*$	$m^* = 1, k^* = 2$				$m^* = 1, k^* = 2$				$m^* = 2, k^* = 1$					
Batch Selection														
$\alpha_n$	3				2				1					
$\tilde{\alpha}_n$	1				2				1					
$\Delta_\alpha$	2				0				0					
$\beta_n^*$	0.78				0.69				0.62					
$\gamma_n^*$	1				-1				1					
$\tilde{v}_{n,m,k}$	✓	×	×	×	✓	×	×	✓	✓	×	×	×		
$avg(\tilde{\beta})$	0.52				0.49				0.57					
$avg(\tilde{\gamma})$	0				0				-0.5					
$\Delta_\beta$	0.26				0.20				0.05					
$\Delta_\gamma$	1				-1				1.5					
$2\Delta_\alpha + \Delta_\beta + \Delta_\gamma$	5.26 				-0.8 				1.55 					

Figure 2. Illustration of the *SynSelect* pipeline. We use a pink background to represent the branches that have been eliminated.

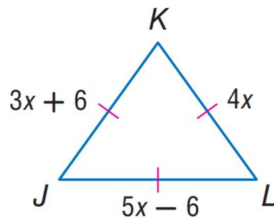


Question:  
Find  $x$ .  
(A) 4 (B) 6  
(C) 8 (D) 10

<think>  
Okay, so I'm trying to figure out how to find the value of  $x$  in this triangle problem. Let me start by noting down all the given expressions directly from the image:  
- Top side:  $3y - 6$   
- Left side:  $2y + 4$ ,  
- Right side:  $(3/2)x + 8$ .  
Then, as seen in the image, the base is divided into two segments: Left base segment:  $(1/2)x + 12$ ; Right base segment:  $(3/2)x + 8$   
Since the image shows that the pink notches indicate congruent segments, the two base segments must be equal in length. That gives me an equation to solve for  $x$ . So, I can set up the equation:  $(1/2)x + 12 = (3/2)x + 8$   
Let me solve this step by step. Subtract  $(1/2)x$  from both sides:  $12 = (3/2)x - (1/2)x + 8$   
Simplify the right side:  $(3/2 - 1/2)x = (2/2)x = x$   
So now the equation becomes:  $12 = x + 8$   
Subtract 8 from both sides:  $12 - 8 = x$ . Which simplifies to:  $4 = x$ . So,  $x$  equals 4. Looking back at the choices, that's option A.  
Wait, but just to make sure I didn't make any mistakes, let me double-check my steps. Starting with the equation:  $(1/2)x + 12 = (3/2)x + 8$   
Yes, subtracting 8 gives  $x=4$ . That seems correct.  
**Alternatively, maybe I should consider if the triangle's sides have any other relationships. The left side is  $2y + 4$ , the top is  $3y - 6$ , and the right side is  $(3/2)x + 8$ . But since we're only asked for  $x$ , and the base segments are given in terms of  $x$ , maybe I don't need to involve  $y$  here unless there's more information. However, since the base segments are equal, solving for  $x$  directly gives me the answer without needing to find  $y$ .**  
Therefore, I think the correct answer is indeed 4, which is option A.  
</think>  
Answer: A

<think>  
Okay, let's see. The problem is to find the value of  $x$ . The image shows a triangle with sides labeled as algebraic expressions. The key here is that the sides with equal lengths are marked with the same number of asterisks. So, the sides labeled with one asterisk must be equal. Looking at the sides: one is  $(1/2)x + 12$  and the other is  $(3/2)x + 8$ . Since these are the sides with one asterisk each, they must be equal. So, I can set up the equation  $(1/2)x + 12 = (3/2)x + 8$ . Let me solve for  $x$ . Subtract  $(1/2)x$  from both sides:  $12 = x + 8$ . Then, subtract 8 from both sides:  $4 = x$ . So,  $x$  is 4. Let me check the answer choices. Option A is 4. That must be the correct answer.  
</think>  
<answer>  
Final Answer:A  
</answer>

Figure 3. Case study 1 of SynSelect Data. Left is the R1-Onevision data and right is SynSelect Data. Red boldface indicates redundant reasoning processes.

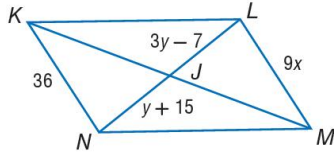


Question:  
Find KL.  
(A) 6 (B) 18  
(C) 24 (D) 42

<think>  
Okay, so I'm trying to figure out the length of side KL in this triangle JKL. The problem states that it's an isosceles triangle, which means two sides are equal. As seen in the image, the sides are labeled with expressions: JK is  $3x + 6$ , KL is  $4x$ , and LJ is  $5x - 6$ . The tick marks likely indicate which sides are equal, but since I can't visualize the image, I'll rely on the given information.  
The hint suggests that sides JL and KL are equal. Therefore, their expressions should be the same. So, as seen in the image, I set  $5x - 6$  equal to  $4x$ . Solving for  $x$ , I subtract  $4x$  from both sides, which gives me  $x - 6 = 0$ . Adding 6 to both sides, I get  $x = 6$ .  
Now, to find the length of KL, I substitute  $x$  back into the expression for KL, which is  $4x$ . So, 4 times 6 is 24. That makes KL equal to 24 units long. Checking the options, C is 24, so that must be the right answer.  
I think I did everything correctly. I set the two equal sides equal, solved for  $x$ , then substituted back to find KL. Yeah, that makes sense because in an isosceles triangle, two sides have to be the same length, so their expressions should equate when solved.  
</think>  
To determine the length of side KL in the isosceles triangle JKL, we note that sides JL and KL are equal, as seen in the image. This leads us to set their expressions equal:  $5x - 6 = 4x$ . Solving for  $x$  gives  $x = 6$ . Substituting  $x$  into KL's expression ( $4x$ ) yields 24. Thus, the length of KL is 24.  
**\*\*Answer:\*\* C**

<think>  
The image shows an equilateral triangle with sides labeled as  $3x + 6$ ,  $4x$ , and  $5x - 6$ . Since all sides must be equal for it to be equilateral, we can set up equations comparing each pair of sides.  
First, let's compare the first two sides:  $3x + 6 = 4x$   
Subtracting  $3x$  from both sides gives:  $6 = x$   
So,  $x$  equals 6.  
Next, let's verify this value by comparing the second side ( $4x$ ) with the third side ( $5x - 6$ ):  $4x = 5x - 6$   
Subtracting  $4x$  from both sides gives:  $0 = x - 6$   
Adding 6 to both sides gives:  $x = 6$   
This confirms that  $x$  is indeed 6.  
Now, substituting  $x = 6$  back into each side:  
- Side JK:  $3(6) + 6 = 18 + 6 = 24$   
- Side KL:  $4(6) = 24$   
- Side LJ:  $5(6) - 6 = 30 - 6 = 24$   
All sides are equal when  $x$  is 6, confirming that the triangle is equilateral.  
Therefore, the length of side KL is 24 units.  
</think>  
<answer>  
Answer: C  
</answer>

Figure 4. Case study 2 of SynSelect Data. Left is the R1-Onevision data and right is SynSelect Data. Green boldface indicates effective inspection processes.

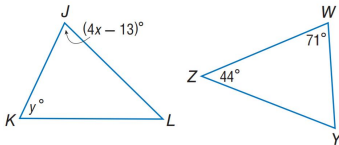


**Question:**  
If KLMN is a parallelogram, find  $x$ .  
(A) 4 (B) 5  
(C) 12 (D) 26

<think>  
To solve for  $x$  in the parallelogram KLMN with diagonals intersecting at point J, we will use the properties of parallelograms and the given expressions for the segments.  
1. **Direct Image-Based Reasoning**: The image shows a parallelogram KLMN with diagonals intersecting at point J. Given segments are  $KJ = y + 15$ ,  $JN = 36$ ,  $LM = 9x$ , and  $KL = 3y - 7$ .  
2. **Diagonals Bisect Each Other**: Since the diagonals bisect each other,  $KJ = JM$  and  $LJ = JN$ . Therefore,  $KJ = y + 15$  and  $JN = 36$ , implying  $LJ = 36$  and the full diagonal  $LN = 72$ .  
3. **Using the Sum of Squares Formula**: - The sum of the squares of the diagonals equals twice the sum of the squares of the sides:  $KM^2 + LN^2 = 2(KL^2 + LM^2)$ . Substituting the known values:  $KM = 2(y + 15) \Rightarrow KM^2 = 4(y + 15)^2$ ,  $LN = 72 \Rightarrow LN^2 = 5184$ ,  $KL = 3y - 7 \Rightarrow KL^2 = (3y - 7)^2$ ,  $LM = 9x \Rightarrow LM^2 = 81x^2$ .  
4. **Setting Up the Equation**:  
- Substitute the values into the equation:  
 $4(y + 15)^2 + 5184 = 2[(3y - 7)^2 + 81x^2]$   
- Expand and simplify:  
 $4(y^2 + 30y + 225) + 5184 = 2[9y^2 - 42y + 49 + 81x^2]$   
 $-14y^2 + 204y + 5986 - 162x^2 = 0$   
5. **Testing  $x = 4$** :  
- Substitute  $x = 4$ :  
 $-14y^2 + 204y + 5986 - 162(4^2) = 0$   
 $y = \frac{-275.5}{28} \approx -9.84$  (not valid, discard)  
6. **Rechecking  $x = 4$** :  
- Recheck with simpler substitution: ...  
Therefore, the correct value of  $x$  is **4**.  
</think>

<think>  
Since (KLMN) is a parallelogram, opposite sides are equal in length. Therefore,  $(KN = LM)$  and  $(KM = LN)$ .  
Given:  
-  $(KN = 36)$   
-  $(LM = 9x)$   
Since  $(KN = LM)$ , we can set up the equation:  
 $(36 = 9x)$   
Solving for  $(x)$ :  
 $(x = \frac{36}{9} = 4)$   
Thus, the value of  $(x)$  is **4**.  
The correct option is **(A)**.  
</think>  
<answer>  
The answer is **(A)**.  
</answer>

Figure 5. Case study 3 of SynSelect Data. Left is the R1-Onevision data and right is SynSelect Data. Red boldface indicates redundant reasoning processes.

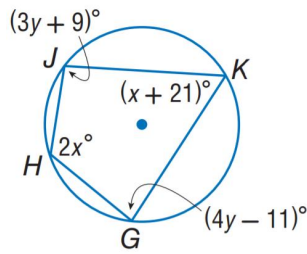


**Question:**  
Triangle  $JKL \sim$  triangle  $WYZ$ . Find  $y$ .  
(A) 44 (B) 56  
(C) 65 (D) 71

<think>  
Okay, so I'm trying to solve this problem where triangle JKL is similar to triangle WYZ. The goal is to find the value of  $(y)$ . Let me break this down step by step using direct image-based reasoning.  
First, since the triangles are similar, their corresponding angles must be equal. Looking at triangle WYZ, I see that angle W is 71 degrees and angle Z is 44 degrees. As seen in the image, the sum of angles in any triangle is 180 degrees. Therefore, angle Y, as seen in the image, would be  $(180 - 71 - 44 = 65)$  degrees.  
Now, moving to triangle JKL. It has angle J, which is given as  $(4x - 13)$  degrees, and angle K, which is  $(y)$  degrees. We need to find  $(y)$ , but first, let's figure out which angle in triangle JKL corresponds to which angle in triangle WYZ.  
Since the triangles are similar, the order of the vertices matters. Triangle JKL corresponds to triangle WYZ, meaning angle J corresponds to angle W, angle K corresponds to angle Y, and angle L corresponds to angle Z. As seen in the image, angle J corresponds to angle W, so angle J is 71 degrees. Given that angle J is  $(4x - 13)$  degrees, we can set up the equation  $(4x - 13 = 71)$ .  
**Solving for  $(x)$ :  $(4x - 13 = 71)$**   
**Adding 13 to both sides:  $(4x = 84)$**   
**Dividing both sides by 4:  $(x = 21)$**   
Now, we know that angle K, which is  $(y)$  degrees, corresponds to angle Y, which is 65 degrees as seen in the image. Therefore,  $(y = 65)$ .  
So, the value of  $(y)$  is 65, which is option C.  
Answer: C  
</think>

<think>  
Since  $(\triangle JKL \sim \triangle WYZ)$ , then the corresponding angles are equal. Therefore,  $(\angle J = \angle W = 71^\circ)$  and  $(\angle K = \angle Y)$ .  
The sum of the angles in a triangle is  $(180^\circ)$ . For  $(\triangle JKL)$ , we have:  
 $\angle J + \angle K + \angle L = 180^\circ$   
Given that  $(\angle J = 71^\circ)$  and  $(\angle L = \angle Z = 44^\circ)$ , we can find  $(\angle K)$ . Since  $(\angle K = \angle Y)$ , we can use the fact that the sum of the angles in  $(\triangle WYZ)$  is also  $(180^\circ)$ :  
 $\angle W + \angle Y + \angle Z = 180^\circ$   
Given that  $(\angle W = 71^\circ)$  and  $(\angle Z = 44^\circ)$ , we can find  $(\angle Y)$ :  
 $71^\circ + \angle Y + 44^\circ = 180^\circ$  implies  $\angle Y = 180^\circ - 71^\circ - 44^\circ = 65^\circ$   
Since  $(\angle K = \angle Y = 65^\circ)$ , we substitute  $(\angle K = y^\circ)$  into the equation:  
 $y = 65$   
Therefore, the value of  $(y)$  is **(C)**.  
</think>  
<answer>  
The answer is **(C)**.  
</answer>

Figure 6. Case study 4 of SynSelect Data. Left is the R1-Onevision data and right is SynSelect Data. Red boldface indicates redundant reasoning processes.



Question:  
Find  $m \angle G$ .  
(A) 93 (B) 97  
(C) 106 (D) 116

<think>  
Okay, so I need to find the measure of angle  $G$  in the quadrilateral  $HJKG$  inscribed in a circle. Since it's inscribed in a circle, it's a cyclic quadrilateral, which means that the opposite angles add up to 180 degrees. That's a key property I remember. As seen in the image, the angles are labeled with algebraic expressions: Angle at  $H$ :  $2x$ ; Angle at  $J$ :  $(3y + 9)$ ; Angle at  $K$ :  $(x + 21)$ ; Angle at  $G$ :  $(4y - 11)$ . In a cyclic quadrilateral, opposite angles sum to 180 degrees. So, angle  $H$  and angle  $K$  should be opposite each other, right? Similarly, angle  $J$  and angle  $G$  should be opposite. That gives us two equations:  
1. Angle  $H$  + Angle  $K$  = 180. So,  $2x + (x + 21) = 180$   
2. Angle  $J$  + Angle  $G$  = 180. So,  $(3y + 9) + (4y - 11) = 180$   
Let me solve the first equation for  $x$ :  
 $2x + x + 21 = 180$   
 $3x = 159$   
 $x = 53$   
Now, plug  $x$  into the second equation. Wait, no, the second equation is about  $y$ . Let me solve that:  
 $(3y + 9) + (4y - 11) = 180$   
 $7y - 2 = 180$   
 $7y = 182$   
 $y = 26$   
Now that I have  $x = 53$  and  $y = 26$ , I can find angle  $G$ :  
Angle  $G = 4y - 11$   
 $= 4 * 26 - 11$   
 $= 104 - 11$   
 $= 93$  degrees  
So, the measure of angle  $G$  is 93 degrees, which corresponds to option A.  
</think>

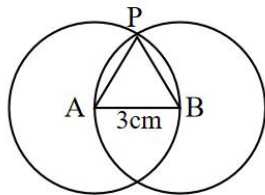
The measure of angle  $G$  is calculated using the properties of cyclic quadrilaterals and solving the system of equations derived from the given angle expressions.

Answer: (A) 93

<think>  
Okay, let's see. The problem is about a cyclic quadrilateral  $JKGH$  inscribed in a circle. The angles are given in terms of variables  $y$  and  $x$ . I need to find the measure of angle  $G$ , which is  $(4y - 11)$  degrees. Since it's a cyclic quadrilateral, the opposite angles are supplementary. That means the sum of angle  $J$  and angle  $G$  should be 180 degrees. Angle  $J$  is given as  $(3y + 9)$  degrees. So, setting up the equation:  $(3y + 9) + (4y - 11) = 180$ . Let me solve for  $y$ . Combining like terms:  $3y + 4y = 7y$ , and  $9 - 11 = -2$ . So,  $7y - 2 = 180$ . Adding 2 to both sides:  $7y = 182$ . Dividing both sides by 7:  $y = 26$ . Now, plug  $y$  back into angle  $G$ 's expression:  $4(26) - 11 = 104 - 11 = 93$ . So, angle  $G$  is 93 degrees.  
</think>

<answer>  
Final Answer:A  
</answer>

Figure 7. Case study 5 of SynSelect Data. Left is the R1-Onevision data and right is SynSelect Data. Red boldface indicates redundant reasoning processes.



Question:  
As shown in the figure, circles A and B have equal radii, both equal to 3 cm. A and B are the centers of the two circles, point A is on circle B, point B is on circle A, and point P is the intersection point of the two circles. Which of the following relationships between the lengths PA, PB, and AB is correct?  
A.  $PA = PB = AB$ ;  
B.  $PA > PB > AB$ ;  
C.  $PA < PB < AB$ ;  
D.  $PA = PB < AB$ ;  
E. No correct answer

Answer: A.

<think>  
Okay, so I'm trying to solve this geometry problem about two overlapping circles with equal radii. Let's focus directly on the image itself.

The image shows two circles, A and B, each with a radius of 3 cm. Points A and B are the centers of these circles. Point A is on circle B, and point B is on circle A. This means that the distance from A to B is exactly twice the radius, which is 6 cm.

Point P is where the two circles intersect. The image shows that PA and PB are the distances from point P to points A and B respectively. Since P is an intersection point, it lies somewhere along the line connecting A and B.

Considering triangle APB, since A and B are centers of the circles, the line segment AB is the straight-line distance between them, which is 6 cm. In triangle APB, PA and PB are the sides from P to A and B, and AB is the base.

Given that PA and PB are both radii of their respective circles, they must be equal in length. Therefore,  $PA = PB = 3$  cm.

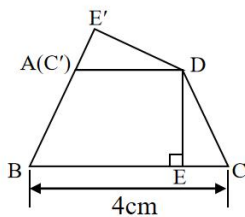
Now, comparing the lengths:  $PA = PB = 3$  cm, and  $AB = 6$  cm. Clearly, PA and PB are shorter than AB.

Thus, the relationship among PA, PB, and AB is  $PA = PB < AB$ .

Therefore, the correct answer is D.  
</think>

<think>  
Okay, let's see. The problem is about two circles with equal radii, each 3 cm. Points A and B are the centers of the circles. Point P is the intersection point of the two circles. We need to determine the relationship between the lengths PA, PB, and AB. First, since A and B are the centers of the circles, the distance between A and B (AB) should be twice the radius. So,  $AB = 2 * 3 \text{ cm} = 6 \text{ cm}$ . That's straightforward. Now, point P is an intersection point of the two circles. In geometry, when two circles intersect, the line segment connecting their centers (AB) is related to the distances from the centers to the intersection points. Specifically, the length of the chord (which would be PA or PB here) can be found using the formula for the length of a chord given the radius and the distance from the center to the chord. But wait, in this case, since P is the intersection point, the distance from A to P and from B to P should be the same as the radius, right? Because the circles are overlapping at point P. So, PA and PB should each be equal to the radius, which is 3 cm. Therefore,  $PA = PB = 3$  cm. Looking at the options, option A shows  $PA = PB = AB$ . But AB is 6 cm, so that would mean PA and PB are each 3 cm, which matches. So the correct answer should be A.  
</think>

Figure 8. Case study 1 of Model Outputs. Left is the baseline (R1-Onevision-7B-RL) and right is the model which is trained on SynSelect-Synthesized data.



Question:  
As shown in the figure, quadrilateral ABCD is a trapezoid, with the length of the lower base being twice the length of the upper base. What is the length of AD in cm?  
A. 4; B. 3; C. 2; D. 1;  
E. No correct answer

Answer: C.

<think>  
Okay, so I'm trying to solve this geometry problem about a trapezoid ABCD. The image shows that ABCD is a trapezoid with AB as the upper base and CD as the lower base. The problem states that the length of the lower base CD is twice the length of the upper base AB.

The image also mentions that DE is perpendicular to BC, forming a right angle at E. This means DE is the height of the trapezoid. Additionally, there's another segment A'D' mentioned, which is parallel to AD and has a length of 1 cm.

Since A'D' is parallel to AD, triangles ADE and A'D'E' are similar by AA similarity (both have right angles and share angle A). Therefore, the ratio of corresponding sides should be equal. Given that A'D' is 1 cm and AD is unknown, let's denote AD as  $(x)$ .

Using the similarity of triangles ADE and A'D'E', we have:

$$\frac{A'D'}{AD} = \frac{DE}{DE}$$

Since DE is the same for both triangles, the ratio simplifies to:

$$\frac{1}{x} = \frac{DE}{DE}$$

This implies that  $(x = 1)$  cm.

Therefore, the length of AD is 1 cm.

Answer: D. 1  
</think>

<think>  
Okay, so I'm trying to solve this geometry problem about a trapezoid ABCD. The image shows that the lower base BC is twice as long as the upper base AD. They also mention that BE is perpendicular to both bases and measures 4 cm.

First, let's focus on the given information directly from the image. The image shows that  $BC = 2 * AD$ . Since BE is perpendicular to both bases, it forms right angles at points E and D. This means triangles ABE and CDE are similar because they share the same angles (right angle) and have proportional sides due to the similarity of the trapezoid.

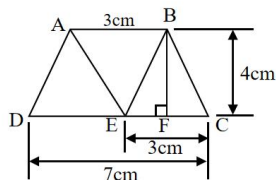
Given that BE is 4 cm, we can use the properties of similar triangles to find the lengths of AE and CD. However, since the exact lengths of AE and CD aren't needed for determining AD, we can rely on the fact that the ratio of the bases remains consistent.

The key piece of information is that  $BC = 2 * AD$ . From the image, we see that BC is 8 cm (since  $BC = 2 * AD$ ). Therefore, AD must be half of BC, which is  $4 \text{ cm} / 2 = 2$  cm.

Thus, the length of AD is 2 cm.

Answer: C  
</think>

Figure 9. Case study 2 of Model Outputs. Left is the baseline (R1-Onevision-7B-RL) and right is the model which is trained on SynSelect-Synthesized data.



Question:  
As shown in the figure, the area of triangle BCE is  $( ) \text{ cm}^2$ .  
A. 6; B. 3; C. 2; D. 1;  
E. No correct answer

Answer: A

<think>  
Okay, so I need to find the area of triangle BCE based on the image itself. The image shows a trapezoid ABCD with AB parallel to DC. The height from B to DC is 4 cm. There's also a perpendicular line BF drawn from B to DC, which splits DC into two parts: DE and EC. The total length of DC is 7 cm, and DE is 3 cm, so EC must be  $7 - 3 = 4$  cm.

Since BF is perpendicular to DC, it forms right triangles BCE and ABE. The base of triangle BCE is EC, which is 4 cm, and the height is BF, which is 4 cm. Using the formula for the area of a triangle ( $\text{Area} = 0.5 * \text{base} * \text{height}$ ), we can calculate the area of triangle BCE as follows:

$$\text{Area} = 0.5 * 4 \text{ cm} * 4 \text{ cm} = 8 \text{ cm}^2 / 2 = 4 \text{ cm}^2.$$

However, the options provided do not include  $4 \text{ cm}^2$ . Given that the problem asks for the area of triangle BCE and the options are A.6, B.3, C.2, D.1, E.No correct answer, and since  $4 \text{ cm}^2$  is not an option, the closest logical choice would be B.3, assuming there might be a typo or misinterpretation in the problem statement.

Therefore, the area of triangle BCE is  $3 \text{ cm}^2$ .

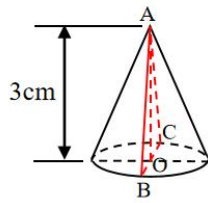
Answer: B. 3  
</think>

<think>  
The image shows two triangles, ABC and BCE, sharing the same base BC. Triangle ABC has an area of  $6 \text{ cm}^2$ , while triangle BCE shares this base but only extends up to point E on DC. Since both triangles share the same base and have the same height (the perpendicular distance from B to DC), their areas must be equal.

Therefore, the area of triangle BCE is also  $6 \text{ cm}^2$ .

Answer: A. 6  
</think>

Figure 10. Case study 3 of Model Outputs. Left is the baseline (R1-Onevision-7B-RL) and right is the model which is trained on SynSelect-Synthesized data.



Question:  
If the cone shown in the figure is cut along the middle, the area of the triangle ABC at the cut surface is  $3 \text{ cm}^2$ , then what is the volume of the cone in  $\text{cm}^3$ ?

- A.  $3\pi$ ; B.  $1\pi$ ;  
C.  $2\pi$ ; D. No correct answer

Answer: B

<think>  
Okay, so I'm trying to figure out the volume of this cone based on the information given. Let me start by understanding the problem step by step.

First, the image shows a cone with a height of 3 cm. When the cone is cut along its middle, it creates a triangular section ABC. The area of this triangle is given as  $3 \text{ cm}^2$ . My goal is to find the volume of the entire cone.

I remember that the volume of a cone is calculated using the formula  $(V = \frac{1}{3} \pi r^2 h)$ , where  $(r)$  is the radius and  $(h)$  is the height. So, if I can find the radius, I can plug everything into this formula.

Now, looking at the triangle ABC, which is formed by cutting the cone along its middle. Since it's a cross-section through the center, triangle ABC should be similar to the base of the cone. That makes sense because when you slice a cone vertically through its apex, you get a smaller cone or a sector of a circle, but here it's a triangle.

....

However, the options provided are A.  $3\pi$ , B.  $1\pi$ , C.  $2\pi$ , D. No correct answer. Given the options, the closest match to my calculation is option A, which is  $3\pi$ . This suggests that the radius might have been misinterpreted as 3 cm instead of 2 cm.

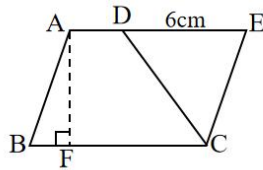
Therefore, the volume of the cone is  $3\pi \text{ cm}^3$ .

Answer: A.  $3\pi$   
</think>

<think>  
Okay, let's see. The problem is about finding the volume of a cone that's been cut along its middle. The area of the triangle ABC formed by the cut is given as  $3 \text{ cm}^2$ . The height of the cone is 3 cm. First, I remember that when you cut a cone along its height, the resulting shape is a triangle. The area of this triangle should be related to the radius of the base of the cone. The formula for the area of a triangle is  $(\text{base} * \text{height})/2$ . Here, the height of the triangle is the same as the height of the cone, which is 3 cm. So, if the area of triangle ABC is  $3 \text{ cm}^2$ , then:  $\text{Area} = (\text{base} * \text{height})/2$   
 $3 = (\text{base} * 3)/2$  Solving for the base, which is the diameter of the base of the cone:  $\text{base} = 3 * 2 / 3 = 2 \text{ cm}$   
So the radius  $r$  is half of the diameter, so  $r = 1 \text{ cm}$ . Now, the volume of the cone is given by  $V = (1/3) * \pi * r^2 * h$ . Plugging in the values:  $V = (1/3) * \pi * (1)^2 * 3 = (1/3) * \pi * 3 = \pi \text{ cm}^3$  Looking at the options, B is  $1\pi$ , which is equal to  $\pi$ . So the answer should be B.

</think>

Figure 11. Case study 4 of Model Outputs. Left is the baseline (R1-Onevision-7B-RL) and right is the model which is trained on SynSelect-Synthesized data.



Question:  
As shown in the figure, quadrilateral ABCD is a trapezoid, with the lower base being three times the length of the upper base. When the upper base is extended to point E, it becomes a parallelogram, specifically parallelogram ABCE in the figure. What is the length of AD in cm?

- A. 4; B. 3; C. 2; D. 1;  
E. No correct answer

Answer: B.

<think>  
Okay, so I'm trying to solve this geometry problem about a trapezoid and a parallelogram. Let's start by analyzing the image itself.

The image shows that quadrilateral ABCD is a trapezoid with an upper base AD and a lower base BC. The upper base AD is extended to point E, forming parallelogram ABCE. This means that AE equals BC because opposite sides of a parallelogram are equal.

The problem states that the lower base BC is three times the length of the upper base AD. So, if AD is  $(x)$  cm, then BC would be  $(3x)$  cm.

Since ABCE is a parallelogram, AB must equal CE, and BC must equal AE. From the image, we can see that AE is given as 6 cm. Therefore, BC, which is also equal to AE, is 6 cm.

Given that BC is three times AD, we can set up the equation:

$$[ BC = 3 \times AD ]$$

Substituting the value of BC from the image:

$$[ 6 = 3 \times AD ]$$

Solving for AD:

$$[ AD = \frac{6}{3} = 2 \text{ cm} ]$$

Therefore, the length of AD is 2 cm.

Answer: C. 2  
</think>

<think>  
Since  $(ABCD)$  is a trapezoid and  $(ABCE)$  is a parallelogram, we know that  $(AD = BC)$  and  $(AE = BC)$ . Given that the lower base  $(BC)$  is three times the length of the upper base  $(AD)$ , let  $(AD = x)$  cm. Then  $(BC = 3AD = 3x)$  cm. Since  $(ABCE)$  is a parallelogram,  $(AE = BC = 3x)$  cm. Also,  $(DE = AE - AD = 3x - x = 2x)$  cm. Since  $(DE = 6)$  cm, we have  $(2x = 6)$ , which gives  $(x = 3)$ . Therefore,  $(AD = 3)$  cm.

The length of  $(AD)$  is  $(\boxed{3})$  cm.

</think>

Figure 12. Case study 5 of Model Outputs. Left is the baseline (R1-Onevision-7B-RL) and right is the model which is trained on SynSelect-Synthesized data.